

# Rock Abrasion Tool

Thomas M. Myrick\*, Kiel Davis\* and Jack Wilson\*

## Abstract

The Rock Abrasion Tool (RAT) is designed to expose the interior of Martian rocks for identification and analysis. The RAT, contained within a cylinder 128-mm long and 85-mm in diameter, has a mass of 687 grams. Using three small DC brushed motors, the RAT grinds a 5-mm deep, 45-mm diameter hole into a targeted rock. During grinding, the grinding wheel, shaped as a paddle with a synthetic diamond-impregnated resin, engages a target rock when the Z-axis is extended. Unrealized during testing, under Mars conditions the grinding wheel wear rate decreases five fold when compared to operation under Earth conditions. In total, four Rock Abrasion Tools were manufactured, two flight units, and two engineering test units. After delivering the flight units, the motor current measured by the RAT's electronic interface did not provide a true reading. Follow-on testing permitted correlating the erroneous data with proper data. The flight units were installed on two separate spacecrafts for delivery to Mars in 2004.

## Introduction

The Rock Abrasion Tool (RAT) is a critical subsystem of the Athena science payload. Designed to mimic the effect of a geologist's hammer, the RAT is used to expose a rock's interior for identification and analysis. Martian rocks cannot be thoroughly examined from the outside because of dust and oxidation. Consequently, from a surface view, most Martian rocks appear visually similar.

To effectively grind rocks on Mars, several key characteristics are required, primarily a desirable cutting material, enough power and force reaction while working, and knowledge of the target material. The first two requirements, cutting material and power and force can be researched and tested; however, information pertaining to the Martian rock composition was illusive prior to the successful use of the RAT. During the design phase, the behavior of Martian rocks with regards to cutting or grinding was not known and had to be estimated leading to complications in deriving our force and torque margins. Throughout the iterative RAT design process various discoveries provided critical knowledge on the development of drilling and grinding units for use on non-Earth planetary bodies. Particularly, important findings were made with regards to the grinding wheel development, the diamond abrasive material.

## RAT Overview

The RAT is designed to grind a 5-mm deep and 45-mm diameter hole into rocks so that science instruments can view the rock's interior. The grinding depth is selectable within the range of the RAT's Z-axis and the topography of the rock surface. The typical command depth is 5 mm. A small rotating brush (Figure 3, label 7) can be used to clean a rock's surface without grinding. Through this method, a rock can be studied with a suite of instruments before and after the surface has been swept clean or grinded.

The RAT (Figure 3), 128-mm long, is contained within a circle 85-mm in diameter, and has a mass of 685 g. It is made primarily from a low density, high modulus alloy of aluminum and beryllium called Albemet, which has a coefficient of thermal expansion similar to steel. Other structural materials include aluminum (7075 and 6061), steel (Vascomax C-250, 4140, 302, 303, 440C, A286, Nitronic 60) and titanium (6AL4V), Vespel, Nickel and 18-karat yellow gold. All of the bearings and gears are lubricated with a grease plate application of Braycote 600 EF micronic and are sealed with Teflon V seals to prevent dust from entering the mechanism. The RAT, using three small DC brushed motors with magnetic encoders, consumes between 8 and 11 watts for a typical three-hour grinding session.

---

\* Honeybee Robotics, New York, NY

The RAT is a stand-alone device in that it does not require any input or movement of the rover's IDD (Instrument Deployment Device) or "arm" once placed onto a rock's surface. The IDD must preload the RAT against the rock within a range of 10 to 100 N. It is desirable for the preload to be at least 50 N for stability. The device's three motors each serve a distinct function and operate in different modes. The RAT grinds a hole in the rock by rotating the grinding wheel (Figure 3, label 2) at approximately 3000 RPM whose center is offset from the center of the RAT by 11.11 mm. The grinding wheel is 23.37 mm in diameter, 6.35-mm wide, and looks like a "paddle wheel" but is referred to as a grinding "wheel". Mounted only along the outer region is a diamond-impregnated resin. The grinding wheel also revolves about the center of the RAT at a very slow speed of 0 - 1 RPM under closed loop control. The combination of high-speed rotate and revolve creates a circular grinding area 45 mm in diameter. The lower half of the RAT housing the grinding wheel is subsequently advanced into the rock in small incremental steps of 0.05 mm per revolution until the desired grinding depth is achieved.

### **Motors**

The grind motor rotates the two shafts at the bottom of the unit where the grinding wheel and the rotate brush, used to remove cuttings from the excavated hole, are attached. These shafts are equally displaced from the center of the housing and centerline of the RAT by 11.11 mm and are therefore separated from each other by a distance of 22.22 mm. This motor operates at a set voltage parameter, typically 27 V, which will rotate the grinding wheel and rotate brush at approximately 3000 RPM. Simultaneously the current provided to the motor is monitored and used as feedback for the grind motor as well as the revolve motor. During mid-day activities, it is typically expected that the bus voltage will be between 28 and 34 V.

The revolve motor causes the revolve housing that supports the two rotate shafts to rotate about a common center point so that the grinding wheel and rotate brush sweep through a full circle 45 mm in diameter. Using a single 45-mm diameter wheel that rotates about the center of the RAT would not be suitable because the velocity of the grinding material at the center of the wheel would effectively be zero, preventing grinding at the center, and therefore halting any advancement of the wheel into the rock. Additionally, with a single wheel approach, removing cuttings would be problematic.

The speed at which the revolve housing rotates is inversely proportional to the grind motor current draw. For example, if a set point of 400 mA of current is commanded for the grind motor, the revolve housing will rotate at its maximum velocity when there is no load on the grind motor as in the case when the grinding wheel is not touching the rock. The maximum velocity of the revolve housing is also a set point that is selectable for each grinding task. Speed constants exist for the revolve motor applied to the grinding algorithm equations. As the current draw from the grind motor increases, the revolve motor slows down to prevent over aggressive cutting into the rock that can lead to stability problems. When the grind motor draws the same amount of current as defined by the current set point, the revolve motor will stop advancing the grinding wheel across the rock until the grind current draw drops when rock material is worn away.

The Z-axis moves the lower section of the RAT in a linear fashion. Extending the axis engages the grinding wheel with the target rock to grind to a user selectable depth. A very high resolution of motion from the Z-axis permits a very small amount of material to be removed with each full revolution of the grinding wheel about the center of the RAT. Attached to a planetary gear head is the motor with an 18.777:1 reduction. A set of spur gears further reduces the rotational output. A 5 mm x 0.5 mm lead screw, coupled to the output of the driven spur gear, provides linear motion.

The Z-axis has a magnetic detent brake built within the upper section of the motor next to the encoder. During launch, landing, or rover traverses the detent brake will prevent the Z-axis from migrating. The detent brake contains four small magnets (Figure 3, label 5) attached to the motor housing that surrounds a steel cross-shaped plate fixed to the motor's rotor. The attraction between the ends of the cross and the magnets acts like a rotation brake that has preferred alignment every 90 degrees. Governed by the gap between the ends of the cross and the magnets, the strength of the brake is designed to hold the shaft

from rotating under worst case loading conditions. However, when motion is desired, the brake is small enough to be overcome by the motor.

Using a predetermined amount of current, the Z-axis position is known through a "Home" routine that drives the lead screw up against a linear jamming hard stop. Afterwards, the lead screw is backed away from the home position by 0.25 mm resulting in the true home position from where all operations start. This hard stop method of positioning the Z-axis was chosen over a switch because of the undesired added real estate and wire count needed for a switch to be used.

### **Brushes**

After grinding, the abraded surface must be free of debris for the microscopic imager, and other instruments on the IDD to accurately view the rock's grain structure and geological properties. For this purpose two fine stainless steel wire brushes are mounted on the RAT, the rotate brush mentioned earlier and a revolve brush fixed to the side of the revolve housing. These two brushes work together in removing dust and cuttings from the hole. The rotate brush removes cuttings from the hole as they are generated and deposits the cuttings atop the perimeter of the excavation site. As the depth of the hole increases, the rotate brush can no longer deposit material atop the increasingly high perimeter of cuttings. This is where the revolve brush aids in the cleaning operation. With every revolution of the revolve housing about the center of the RAT, the revolve brush pushes the building perimeter of material away from the edge of the hole so that the rotate brush can eject the cuttings onto a relatively debris free perimeter. This dual brush action keeps the hole clean and free of material that would otherwise interfere with the quality of data collected by the other instruments. Alternatively, the dual brush action can be used to clean the surface of a rock without grinding. Through this approach any of the science instruments can view a rock's surface dust free.

### **Butterfly Unit**

The lower section of the RAT is made up of a butterfly mount and two butterfly wings that act as a preloading structure between the IDD and the rock. The butterfly assembly is required because the IDD is not stiff enough to suspend the RAT above a rock in a free-floating state and provide reaction forces to counter the grinding process. When the RAT is placed onto a feature of interest, whether it is a rock, duricrust, or blocky soil, the IDD preloads the knurled balls (Figure 3, label 4) of the butterfly wings (Figure 1, label 2) onto the rock. As the RAT engages a surface feature, two switches (Figure 1, label 5) that reside within the butterfly assembly will close when a preload of 5 N is reached. After the switches close, the arm will move further into the rock to establish the commanded preload for grinding. Should the preload drop below 5 N at any point during the grinding operation, possibly as a result of rover or rock movement due to settling, one or both of the switches will open and the software will command the Z-axis to back away from the rock and then re-engage the rock. Should repeated switch openings continue, the result is that the penetration rate will either stop or slow to the point where a revolve timeout flag will appear that will abort the grinding algorithm. This event will be sent to Mission Control along with all other RAT grinding data.

The design of the butterfly elements that engage and become preloaded against a rock was a formidable task. It is necessary to actually preload the ground structure of the RAT against the rock, effectively closing the loop, which will dramatically increase the overall stiffness of the IDD for force reaction. The need to reside the ground structure outside of the grinding area accounts for the design of the butterfly wings. The RAT engages the rock at the bottom surface of each knurled ball mounted to the butterfly wings. These balls have this hemispherical design to allow the wings to freely slide over the rock topography during the approach vector without getting caught on a ledge or vesicle until the preload is established. The pair of butterfly wings is free to rotate +/-16 degrees about the pivot point on the butterfly mount. Additionally, each butterfly wing can move relative to each other by about one degree (for contact switch motion) and have compression springs mounted between the two butterfly wings to provide a spring loaded bias of 5 N applied at the knurled ball area on the wings. In this way, when the butterfly wings are loaded against a rock surface, they will rotate relative to each other by about one degree until the gold switches are closed which also act as hard stops. The wings can accommodate engaging a rock

surface that is not normal to the approach vector because they are free to rotate  $\pm 16$  degrees in the pitch axis. This allows the wings to properly seat themselves against a rock surface so that equal force is applied to each of the wings' knurled balls. The knurled balls can accommodate approach vector errors of  $\pm 15$  degrees in a yaw axis as well because they protrude downward from the frame of each wing. If the rock surface plane is at an angle equal to or greater than  $\pm 16$  degrees in either the pitch or yaw directions, hard stops will prevent the butterfly wings from pivoting further, preventing the switches from closing. Typically, the IDD will present the RAT normal to the local surface plane of the rock at an angle that is within 5 to 10 degrees.

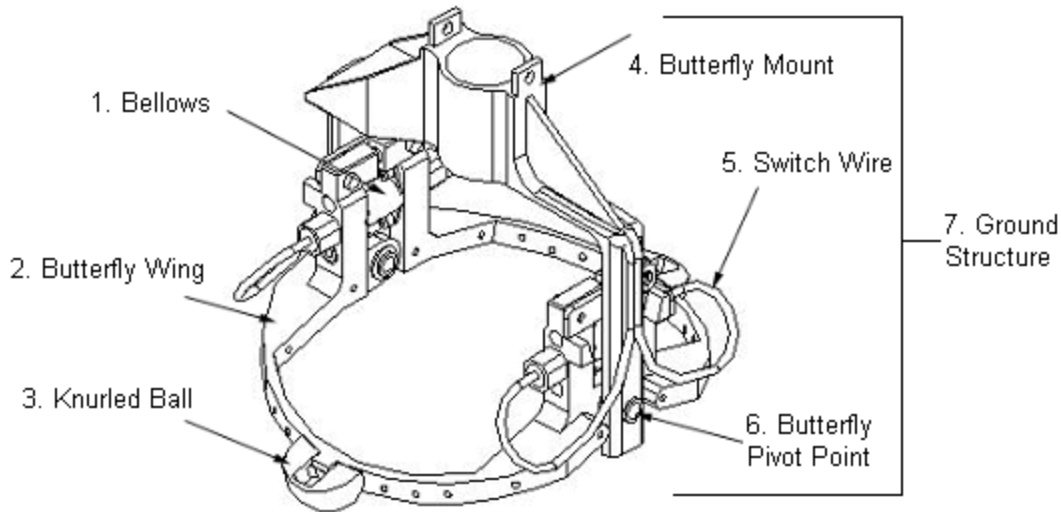


**Figure 1. Rock Abrasion Tool -- Butterfly Isometric View**

The switches were of particular concern due to the imposed requirements. They need to be small enough to fit within the very limited space allotted, they cannot have any hysteresis or dead band characteristics and they have to be dust proof. Additionally, the switches have to act as hard stops capable of withstanding loads as high as 125 N acting at the knurled balls which becomes about 222 N at the gold contacts. All of these requirements lead to designing and manufacturing custom made switches as commercial flight micro-switches could only satisfy the dust proof requirement. The contact material was made from 18-karat full hard yellow gold, which is also strong enough to withstand the relatively high compression loads. The gold contacts are insulated from the structure of the RAT via Vespel bushings. The backside of each switch half is back filled with epoxy at the point where each wire protrudes. This offers strain relief for the wire in addition to added bond strength for the gold and vespel bushing. The exposed gold contact heads are enveloped and sealed using a nickel bellows with custom end plates that are secured to each side of the wings. The breather vent had to be installed to allow trapped air to escape because assembly of the gold contacts (Figure 2, label 1) took place in Earth atmosphere. The vent was made using a stainless steel setscrew that was counter bored and filled with a 316 SS powder that was heated and compressed. This became a 2-micron filter, allowing gasses to exchange and equalize the pressure on both sides of the bellows yet prevent dust from contaminating the gold contacts. Had the breather vent not been installed, the spring constant of the butterfly switch system would have been greater than the 5 N calibration threshold.

Mounted within the bottom of the revolve housing are four small magnets (Figure 3, label 5) with varying degrees of strength. These magnets, provided by scientists from the University of Copenhagen, Denmark, will be used to characterize the magnetic properties of the cuttings produced by the grinding operations. For more information, see [Madsen et al., 2003]. The RAT magnets are designed to capture magnetic particles originating from the grinding of Martian surface rocks. A high-resolution stereo camera called Pancam, developed at Cornell University, will image the magnetic particles captured by these magnets. A major science goal for the Magnetic Properties Experiment (MPE) on the rovers is to identify the mineral(s) responsible for the magnetism of Martian rocks, soil and dust. In addition an effort will be

made to obtain information on the crystallite size of the magnetically ordered Fe (III) compound(s) in the dust.

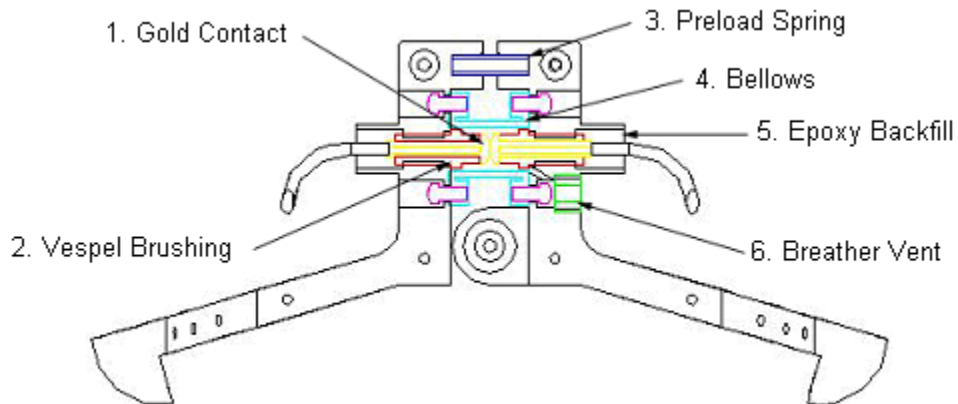


**Figure 2. Rock Abrasion Tool -- Butterfly Switch Section View**

The surface produced by the grinding operation will serve the science interests well. Typically, the surfaced is quite smooth and in some cases it is as smooth as a granite counter top. This clean, smooth surface should enable the microscopic imager to view grain structures and other features of the rock.

### Science Return

In addition to grinding a clean, smooth surface, the RAT can also provide information characterizing the rock's physical properties. By analyzing the data set returned to Earth, the RAT generated data will be compared to information from an extensive collection of rock grinding data generated at Honeybee Robotics and stored in Honeybee's rock library. Other methods of manipulating the data will be used to determine the rock's physical properties. If the amount of material removed is known, the amount of required energy per unit volume of material can be determined. This ratio can then be compared to data within Honeybee's library to determine which type of rock tested on Earth most closely represents the excavated Mars rock, thus providing the rock's physical strength properties.

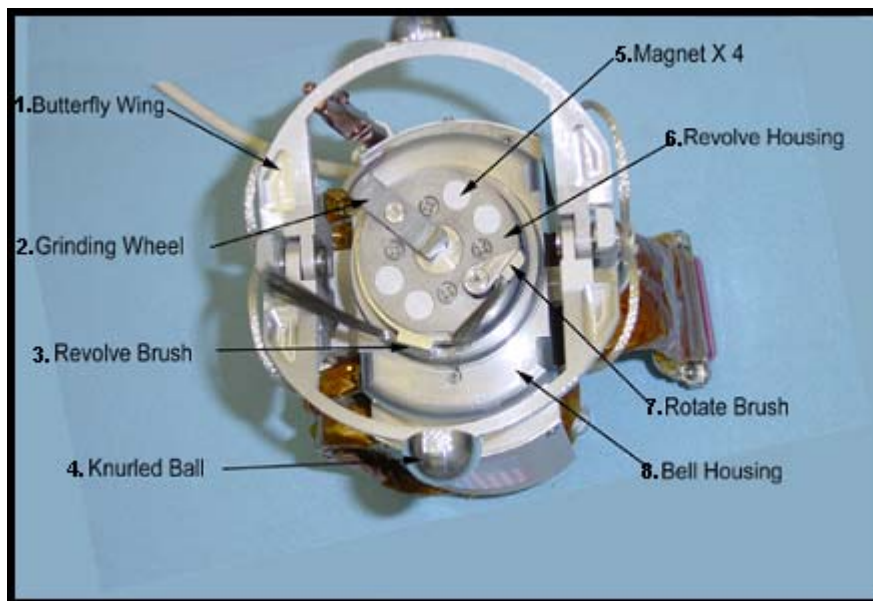


**Figure 3. Rock Abrasion Tool -- Bottom View**

## Cutting Abrasive

A great deal of research, design and testing was conducted as part of the grinding wheel development process. We began our investigation of grinding wheel materials with an emphasis on diamond products. These are the hardest materials available, will operate at relatively high surface speeds and are subjected to low forces where tougher materials are not needed. We experimented primarily with synthetic diamonds, limiting our investigation of natural diamonds. The relatively minor additional hardness of natural diamonds does not outweigh the more predictable and repeatable properties of their synthetic counterparts. We tested large single crystal diamonds faceted to form a rake and relief angle needed for cutting and multiple large and small diamond crystals bonded in a single layer to a steel substrate. In all, we tested at least 50 different material and geometric combinations. Upon investigation we learned that the tips of the diamond grains developed flat spots that prevented further grinding within our bounded force limits. This discovery came as a surprise to us, as the force per grain is quite low and diamonds are much harder than the basalt that we were using as our test standard. These small flats created too much surface area for the low loading of the tool on the rock to have any cutting effect. A diamond abrasive with the ability to self sharpen was needed. In this approach, when the diamond grains wear, they fall out and expose fresh, sharp grains. Resin diamond wheels are designed especially for this purpose. Early testing of resin diamond wheels led to very poor results because whole wheels were used that presented a large surface area to the rock. A second approach, attempted later on, was designed to use resin diamond wheels also with very little down force. In this approach, the wheels were cut along two cords forming two small pads of resin along the perimeter of the "wheel" to engage the rock. Resultantly, the contact area with the rock was reduced, causing a higher force per grain. Ultimately, we settled on a grain size of 100-120 mesh (0.1-mm diameter) and a concentration of 112 (which has a volume of 28 percent diamond). The diamonds were coated with 56 weight percent Nickel that enhances the bond characteristics of the diamond to the resin. The resin is a phenolic with silicon carbide and cryolite fillers. This seemed to be the best formula for grinding within the given parameters. The sacrificial consumption of the grinding pad thickness was about 0.5-0.64 mm (20-25 mils) per grind event in hard rock in Earth atmosphere. This gave us a tool life of about five grindings in strong basalt. We then investigated the geometry of the actual resin diamond pads.

The size and shape of the grinding pads affected the level of success of each grinding experiment in how deep the bit was able to grind as well as how much time and energy was expended. Additionally, how much wear each grinding pad endured was important in the development of the pad design. If the pads were large in terms of surface area contact with the rock, it would see less wear than one of smaller contact area, yet the penetration rate would suffer. Furthermore, the shape of the pads was important in minimizing induced vibration and pad bond integrity with the substrate. The arc length of each pad must be inversely proportional to the width of the pad in order to maintain a given surface area. Through experimentation, we knew that the surface area of each pad must be on the order of 13 square millimeters or less. For vibration concerns, a large arc length would be better but this would make the width of the pads unacceptably thin in terms of bond integrity and manufacturability. Throughout the process of filling in an elaborate testing matrix, we settled on an arc length of 6.35 mm and a width of 1.5 mm. The usable thickness of the resin material is 2.6 mm. This thickness is governed by parameters set earlier in the design that involve among other things, the topography of the rock that can be dealt with and what clearance should be afforded in order to commence the grinding algorithm.

## Force and Torque Margin Analysis

After completing the design of the RAT, we built four units. The first two are labeled Engineering Model 1 (EM1) and Engineering Model 2 (EM2). These units are exactly the same as the flight units but are used for testing here on Earth, EM1 at the Jet Propulsion Laboratory (JPL) and EM2 at Honeybee Robotics. We also built two flight units, Flight Model 1 (FM1) and Flight Model 2 (FM2). FM1 was installed on the Opportunity rover and FM2 was installed on the Spirit rover. FM1 and FM2 underwent Qualification Testing under a range of temperatures and loading conditions at Mars atmosphere. The Electrical Ground Support Equipment (EGSE) used for issuing the test commands and collecting the data products had an anomalous behavior that was not diagnosed until both flight units were delivered. The EGSE can be defined as the set of electronics and software that directly interfaces with the RAT actuators and sensors

and handles RAT control and data acquisition tasks. The problem with the EGSE was the motor current that it measured and stored was not the actual current consumed by the motors. In some cases, the EGSE showed more current than was actually consumed and in other cases, the EGSE showed less current than was consumed. It appeared that the Pulse Width Modulator (PWM) current output was not a linear relationship with respect to the commanded percentage issued to the PWM. As a result, the data collected could not be used to determine the amount of current needed for each motor given various loading and temperature conditions. Furthermore, torque margins could not be assessed based on the information at hand. Since the two flight units had already been delivered, we could not use them to perform a second round of tests with a proper measurement of the motor current. Consequently, we decided to dyno-test the EM2 unit using the same erroneous current collecting EGSE. This allowed us to compare the EM2 unit to the two flight units and make a determination as to whether the EM2 unit was “in family”, meaning the difference in behavior is insignificant, with regard to the two flight units. After completing the same no loads tests, using the erroneous EGSE equipment that were conducted on both flight units, and comparing the data, we concluded that all three units were indeed within “family”. With this understanding, we could then test the EM2 unit under Qualification Test conditions using a correct method of measuring each motor’s current and assess torque margins that we could apply to both flight units. The following is a detailed account of the methods we used in determining if the assembled units behaved the same and the technique of determining motor torque margins for each of the three motors within both flight units.

#### Dynamometer Tests

The purpose of the EM2 RAT actuator dynamometer testing was to characterize the speed-torque-temperature relationships of the RAT actuators including the drive trains, and to verify the ability of the actuator components to survive excursions to extreme temperatures. The additional purpose of dynamometer testing was (1) to determine the closed loop relationship between motor currents required for rock grinding and the actual forces and torques applied, (2) to verify that the performance of EM2, FM1 and FM2 RATs are “in family” and explain any disparities that exist, (3) to determine the torque margin on each actuator at key temperature set points, (4) to determine a set of FM1 and FM2 parameters that are safe for the RAT, but robust enough to successfully grind, and (5) to determine the maximum turn-on time for actuators that exhibit low margin at certain temperatures, using analytical and experimental methods.

#### Closed Loop Motor Current / Torque Relationship

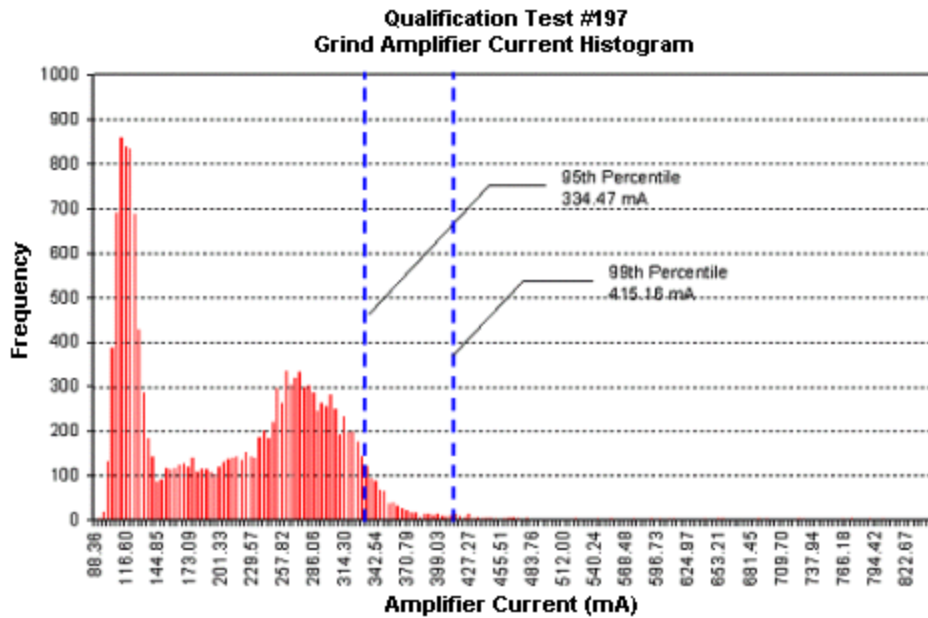
All EM2 RAT motors have been dynamometer tested in order to characterize their current versus torque/force profiles at several different temperatures. Several grinding tests have also been performed with the EM2 RAT at 0°C. These grinding tests represent a worst-case scenario in terms of rock compressive strength and topology and the data was used to determine the worst-case torque and force requirements for all three RAT motors. The rock used for tests was a strong basalt, and the surface topology was flat (no peaks or valleys on the rock) in order to demonstrate the full capability of the RAT. Four grinding tests were performed on basalt, with the RAT at 0°C. These tests are numbered #197 - #200, and will be referred to as such.

#### Rotate (Grind) Motor Analysis

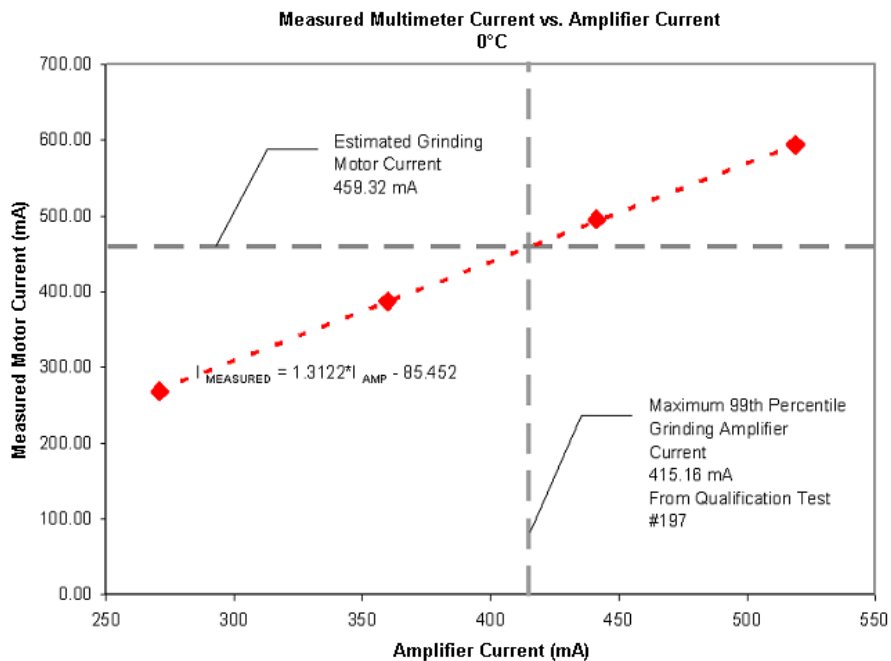
Using the erroneous EGSE data obtained from grinding tests #197 - #200, the amplifier current vs. time was plotted for the grind motor throughout the duration of the test. Occasional “spikes” were observed in the data where the amplifier current would jump much higher than the typical range of values. These spikes occurred over a very short time period and do not negatively affect the performance of the RAT. The peaks in the amplifier current data do not represent the worst-case grinding current because they only occur for very short amounts of time, and only a few times during a typical grind. Therefore, in order to determine the worst-case torque requirement, a statistical approach was taken for the data analysis.

Figure 4 shows a histogram of the grind motor amplifier current during grinding test #197. The vertical dotted lines show where 95 and 99 percent of the amplifier current fall and the resulting value. This approach was taken in order to help filter out some of the anomalous current spikes in the data, and to have a mathematical basis from which to define the current / torque relationship. The 99<sup>th</sup> percentile value of 415.16 mA was used from this test to determine the current / torque relationship for the grind motor.

In order to determine the actual grinding torque based on true motor current, a calibrated multimeter was placed in series with the grind motor during dynamometer testing. This data was then used to convert amplifier current to true motor current. Figure 5 shows the average motor current vs. average amplifier current obtained from dynamometer testing performed at 0°C (same temperature at which grinding was performed). The vertical line shows the 99<sup>th</sup> percentile grind motor amplifier current obtained from the grind motor histogram. The horizontal line shows the corresponding direct motor current of 459.65 mA. This is the worst-case scenario for motor current during grinding.



**Figure 4. Grind Motor Histogram**



**Figure 5. Motor Current vs. Amplifier Current**

Figure 6 shows the motor current vs. torque for the grind motor at 0°C. This graph was obtained using averaged data from the grind motor dynamometer testing. The horizontal line represents the worst-case motor current during grinding, and the vertical line on the left represents the corresponding torque on the motor (25.13 mNm). This is the worst-case torque applied to the grind motor during a grinding operation. This value was used to define the torque requirement for the RAT margins.

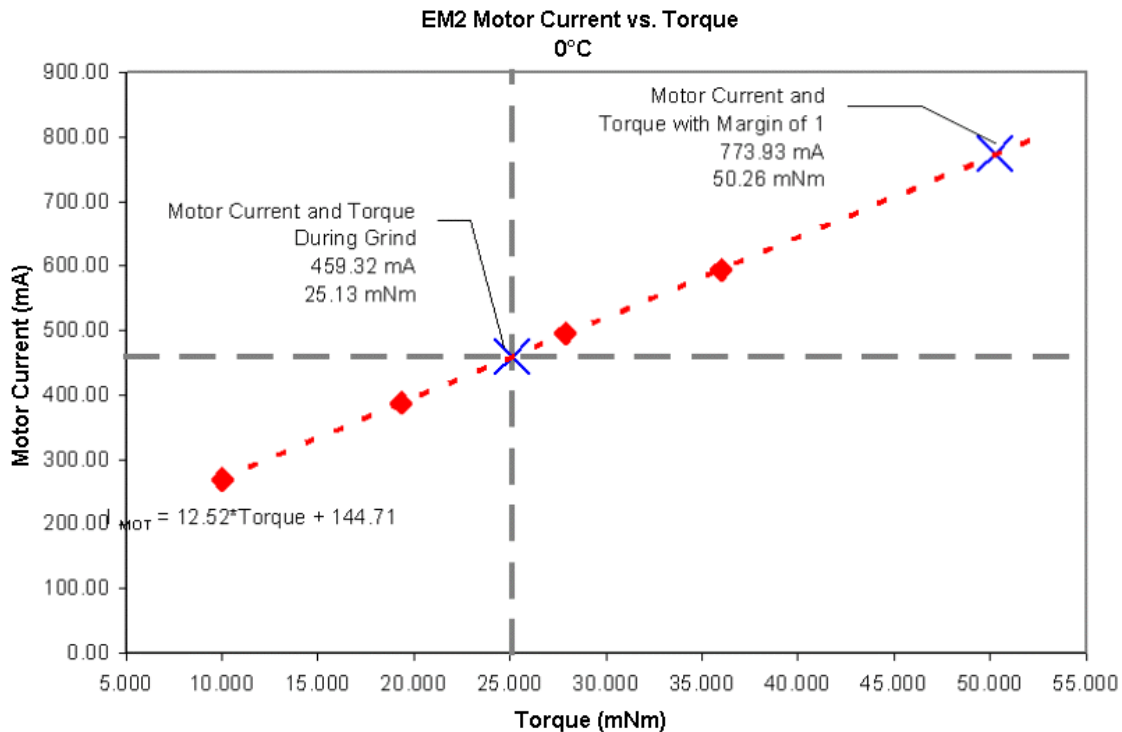


Figure 6. Motor Current vs. Torque at 0°C

#### Revolve Motor Analysis

The closed loop current / torque relationship was determined for the revolve motor similar to how the grind motor was analyzed. The worst-case amplifier current drawn by the revolve motor during a worst case grind was calculated to be 28.29 mA (99<sup>th</sup> percentile). From this value it is estimated that the revolve motor experiences a worst-case torque of 166.6 mNm during a worst-case grinding operation. The revolve motor is heavily geared down mechanically, and the majority of the grinding torque created is due to internal losses. This causes motor margin to be difficult to determine based solely on torque. In order to demonstrate that the action of grinding does not cause significant torque loads on the revolve motor, the amount of torque experienced by the motor with no load attached to it was calculated. To achieve this, the revolve motor was run de-coupled from the dynamometer, and the no-load current was measured. The amplifier current was then interpolated between 3 V and 6 V because the revolve motor typically runs at 4 V during a grinding operation. The heavy gearing of the revolve motor causes a torque of approximately 156.8 mNm, which is only about 10 mNm less than the torque seen during a worst-case grinding operation.

#### Z-Axis Motor Analysis

The closed loop current / torque relationship was determined for the Z-axis motor similar to how the revolve motor was analyzed since both motors are heavily geared down mechanically. The worst-case amplifier current drawn by the Z-axis motor during a worst-case grind was calculated to be 23.8 mA (99<sup>th</sup> percentile). From this value it is estimated that the Z-axis motor experiences a worst-case force of 5.907 N during a worst-case grinding operation. From no-load current values, it is estimated that the heavy gearing of the Z-axis motor causes a force of approximately 4.04 N, which is approximately 2 N less than the force seen during a worst-case grinding operation.

**Table 1. Closed Loop EM2 Motor Current to Force/Torque Relationship Summary**

Motor	Qualification Test #	99th Percentile Amplifier Current	99th Percentile Motor Current	99th Percentile Grinding Torque / Force
Rotate (Grind)	197	415.16 mA	459.32 mA	25.13 mNm
Revolve	199	28.29 mA	41.92 mA	166.6 mNm
Z-axis	197	23.8 mA	29.07 mA	5.907 N

**EM2 RAT Thermal Margin Analysis**Grind Motor

The grind motor performance limits the RAT since it is the motor most likely to overheat. The heating of the grind motor is governed primarily by two variables, (1) the motor current and (2) the ambient temperature. Using the grinding torque found by closing the loop between grinding current and torque (25.13 mNm), the motor current can be found at all temperatures tested. This current, along with the corresponding ambient temperature, was entered into a RE25 motor thermal model in order to determine the time at which the motor will overheat. The temperature limits on the grind motor are +110°C for the rotor and +85°C for the case. At nominal operating torque (25.13 mNm), the motor will overheat in 28 minutes at +55°C. The motor does not overheat at the next lowest temperature tested, +35°C. For this reason, +35°C is specified as the maximum turn-on temperature (MTO). The thermal time limitation was found at a safety factor (SF) of 1.5 and 2.0 (margin of 0.5 and 1.0 respectively). This was done using motor current vs. torque data to find the motor current corresponding to a torque of 37.69 mNm (SF of 1.5) and 50.26 mNm (SF of 2.0). These values for motor current were then applied to the transient thermal model in order to arrive at a time limitation for the motor at margin.

**Table 2. Grind Motor Thermal Margins**

Temp. (°C)	Grind Current Margin of 0 (mA)	Grind Current Margin of 1 (mA)	Time to Overheat (min) for Margin of 0	Time to Overheat (min) for Margin of 0.5	Time to Overheat (min) for Margin of 1
+55	378.7	696.6	28	23.67	9.33
+35	396.3	710.77	Infinite	43.67	14.67
+23	400.83	704.27	Infinite	140.67	20
0	459.32	773.96	Infinite	Infinite	22
-20	471.37	779.3	Infinite	Infinite	31.67
-40	510.65	782.79	Infinite	Infinite	48
-55	539.5	844.45	Infinite	Infinite	41.67
-70	567.98	868.08	Infinite	Infinite	47.67

Revolve Motor

Due to the internal losses in the drive train of the revolve motor, the torque produced by a grinding operation is very small compared to the torque absorbed by the gear reduction. During a grind, the revolve motor has a much lower duty cycle than the grind motor, and for this reason there is no chance for the revolve motor to overheat. This necessitates a different way of determining the torque margin. There are two potential failure modes in the revolve motor's operation, (1) abnormally high internal losses in the drive train, and (2) unexpected areas of highly dense rock. Due to the relatively low contribution to overall torque of the grinding operation, the most probable failure point is within the drive train. Since the torque due to the drive train cannot be measured directly, the torque margin analysis will be based on a no external load motor current, rather than measured torque.

For each thermal test point (+55°C, +23°C, 0°C and -55°C), the motor was run in velocity mode to simulate the required speed that it needs to operate at during a grind (0.35 radians/sec). This was performed while de-coupled from the dynamometer. This no-load motor current was used as the basis for the torque margin since the revolve motor needs to draw at least this amount of current at a certain temperature in order to overcome internal losses in the gear train. To determine the torque margin, the

revolve motor was coupled with the dynamometer and again run in velocity mode at 0.35 radians/sec at each temperature set point. The dynamometer was used to apply a torque load on the motor until the motor current was as close to twice the no-load current as possible. For some temperature set points (0°C and +23°C) it was not possible to produce enough torque to double the no-load current due to the limitation of the dynamometer (maximum applied torque of 350 mNm).

To determine thermal margin, the peak motor current was calculated while running the revolve motor in voltage mode. This current was doubled and used in the RE020 motor thermal model to determine the transient heating of the motor at all temperature set points. It was found that the revolve motor does not overheat at any of the temperature set points or voltages.

**Table 3. Revolve Motor Thermal Margin (RE20 Motor)**

Temp (°C).	Maximum Motor Current (mA) at 3V, 150 mNm	2X Maximum Motor Current (mA) at 3V, 150 mNm	Overheat (min)	Maximum Motor Current (mA) at 6V, 150 mNm	2X Maximum Motor Current (mA) at 6V, 150 mNm	Overheat (min)
+55	34	68	Infinite	35.8	71.6	Infinite
+35	34.3	68.6	Infinite	36.9	73.8	Infinite
+23	36.1	72.2	Infinite	37.5	75	Infinite
0	35.8	71.6	Infinite	40.6	81.2	Infinite
-20	41.3	82.6	Infinite	53.1	106.2	Infinite
-40	67.7	135.4	Infinite	71	142	Infinite
-55	89.4	178.8	Infinite	74.6	149.2	Infinite
-70	142.1	284.2	Infinite	152.9	305.8	Infinite

#### Z-Axis Motor

As with the revolve motor, the force caused by a grinding operation is very small compared to the force absorbed by the gear reduction and friction due to internal losses in the drive train of the Z-axis motor. During a grind, the duty cycle of the Z-axis motor is an order of magnitude lower than that of the grind or revolve motors. For this reason, there is no chance for the Z-axis motor to overheat. The revolve and Z-axis motors share the same potential failure modes during operation. Again, due to the relatively low contribution to overall force of the grinding operation, the most probable failure point is in the drive train. The exact approach used to determine the revolve motor torque margin was also used for the Z-axis motor.

For each thermal test point (+55°C, +23°C, 0°C and -55°C), the motor was run in velocity mode to simulate the required speed that it needs to operate at during a grind (0.05 mm/sec). This was performed while de-coupled from the force controlled air cylinder. The motor was run for close to a full stroke of the output and the resulting motor current was averaged. To determine the torque margin, the Z-axis motor was coupled with the air cylinder and run in velocity mode at 0.05 mm/sec at each temperature set point. The air cylinder was then used to apply a load on the motor until the motor current was as close to twice the no-load current as possible. The maximum force that the load cell can measure accurately is slightly over 50 N (the load cell specification has 50 N as the maximum measurable load; however, it was observed through testing that this is not the absolute limit). For one temperature set point (-55°C) it was not possible to produce sufficient load to double the current because it would have well exceeded the limitation of the load cell.

To determine thermal margin, the peak motor current was calculated from dynamometer testing of the Z-axis motor in voltage mode. This current was doubled and used in the RE020 motor thermal model to determine the transient heating of the motor at all temperature set points. It was assumed that the motor was run constantly rather than intermittently. It was found that the Z-axis motor only overheats at and below -55°C when operating at a voltage of 8 V, with a load of 30 N or more on the motor, and at a safety factor of 2.0. This is well above the expected 4 V operating voltage, and far above the expected 6 N load on the motor during grinding.

**Table 4. Z-Axis Motor Thermal Margin (RE20 Motor)**

Temp (°C).	Maximum Motor Current (mA) at 4V, 30N	2X Maximum Motor Current (mA) at 4V, 30 N	Overheat (min)	Maximum Motor Current (mA) at 8V, 30N	2X Maximum Motor Current (mA) at 8V, 30 N	Overheat (min)
+55	46.6	93.2	Infinite	43	86	Infinite
+35	41.4	82.8	Infinite	39.1	78.2	Infinite
+23	40.2	80.4	Infinite	46.3	92.6	Infinite
0	46.1	92.2	Infinite	52.2	104.4	Infinite
-20	56.7	113.4	Infinite	73.7	147.4	Infinite
-40	100.9	201.8	Infinite	137.8	275.6	Infinite
-55	127.8	255.6	Infinite	172.7	345.4	24.33
-70	167.4	334.8	Infinite	285.1	570.2	2.75

**“In Family” RAT Models**

During the FM1 and FM2 dynamometer test, the methods for measuring motor current were inaccurate. The motor current data recorded during those tests was amplifier current. The true (direct) motor current was measured throughout the EM2 dynamometer tests and it is understood that the motor current is a nonlinear function of amplifier current and PWM duty cycle among other things. Sufficient data does not exist to allow the FM1 and FM2 erroneous motor currents to be transformed to actual motor currents. Therefore, in order to determine that the EM2 is “in family” with the FM1 and FM2, the amplified motor current had to be correlated to the direct motor current. The data shows that all of the actuators in the three units behave similarly at most temperature set points; however, there are a few disparities between the motors, which mostly occur at lower temperatures, -70°C in particular.

Most of the disparities can be attributed to (1) mechanical variations in the motor drive trains (the current obtained from the dynamometer tests include the current due to the internal losses in the drive train, and although all parts are made to same print, there are fitting differences and the lubricated parts can behave differently at cold temperatures), (2) set limits in the control software, and (3) an improper bake out during one test.

Disparities at -70°C:

- The FM1 revolve no-load current at 3 V is much lower than the FM2 and EM2. The FM1 revolve did not move at -70°C because the current reached its limit. When FM1 was tested, increasing current limits at colder temperatures was not considered due to lack of test experience. These limits were increased before FM2 and (subsequently) EM2 were tested.
- The EM2 revolve no-load current at 6V is much higher than the other two units. This is due to the revolve current reaching its upper limit and not moving.
- The Z-axis no-load motor current comparison at 8 V showed that the FM2 current is much higher than the FM1 current and the EM2 current is much higher than the FM2. For FM1 again, increasing the current limits at colder temperatures was not considered, therefore the FM1 Z-axis did not move at -70C because the current limit was reached. This current limit was increased for EM2 testing, but the unit was not properly baked out during the test, so the Z-axis did not move at -70°C because it reached its current limit. The effects of the improper bake out were also apparent at -55°C, where the EM2 Z-axis motor current was running high. However, it was determined that the EM2 Z-axis no-load current is close to that of FM2.

Overall, the differences between the three units at nominal operation temperatures are minor and it is concluded that all three units are “in family”, and so the results from the EM2 Margin Analysis based on the EM2 grinding and dynamometer test data can be applied to FM1 and FM2.

## Lessons Learned

- 1) The delivery schedule of the grinding wheels for integration into the flight assembly was such that we did not have enough time to test the behavior of the diamond resin wheels in a simulated Mars environment prior to delivery. Obviously this is not the way we would have liked to proceed but we had no choice as the delivery deadline was fast approaching as we finished our last round of testing. Later, we were able to test the final wheel design under Mars environmental temperature and pressure. During these tests, we discovered that the wear rate of the diamond/resin decreased dramatically in a simulated Mars environment. Under Earth conditions, the wear rate was about 0.51-0.64 mm per basalt grind event. Under Mars environmental conditions, we saw wear rates of about 0.1-0.127 mm per basalt grind event. This is a five-fold decrease in the wear rate or a five-fold increase in tool life or about 25 basalt grind events. System level requirements imposed a tool life of three grindings with a margin of one (six grindings). In retrospect, if we knew that this wear effect was present, we would have decreased the concentration of diamond in the resin mix. This would have the effect of reducing the tool life through increased wear (something we could live with) and increased the grinding performance of the tool because with fewer stones in the matrix there would be more force per stone, thus increasing the grinding properties.

After learning of this diamond behavior under Mars conditions, a paper written by Hitchiner et al. (1983) from Oxford University provided complementary information. Hitchiner compares the effects of polishing diamond on an iron scribe in Earth atmosphere and at a vacuum of 0.1 Torr. His conclusions describe a five-fold decrease in the wear rate under vacuum. Therefore Mars acts more like a vacuum than Earth atmosphere with regards to diamond wear rates.

- 2) The Z-axis lead screw hard stop should have been designed so that it acted as a rotational hard stop. With small posts projecting upward on the lead screw and a small post projecting downward from the ground structure, this rotational hard stop could have been implemented. It would have given the instrument more repeatable positional information and it would not have depended as heavily on the temperature and thus current limit at which the system is activated.
- 3) The only Platinum Resistive Thermocouple (PRT) that was available to us was mounted on the Z-axis motor with the thought that it would more accurately provide the true morning temperature of the RAT as well as limit the number of wires that must flex while the RAT was in motion. However, in use, it seems that the PRT would be put to better use if it were mounted to the grind motor that has by far the highest duty cycle of all the motors. This would have allowed direct reading of the grind motor's temperature during operation as opposed to a thermal model looking for overheating, which is currently used.
- 4) During the assembly of the RAT engineering and flight models, the 37 pin micro D connectors were backfilled with an epoxy, model # PR-1590, made by PRC Desoto International. Throughout the process of verifying our mixing procedure, testing our Teflon mold, and applying this procedure to the engineering and flight models we learned that the compound was extremely sensitive to atmospheric humidity. If the humidity levels were greater than 30%, the compound formed bubbles that could not be eliminated even when immersed in a vacuum chamber, as part of our procedure designed as a precautionary step to prevent bubble formation. Regardless of the amount of applied vacuum, the bubbles continued to form in the presence of high humidity levels. Ultimately we kept our clean room at or below 30% humidity, yielding successful molds with no bubbles.

## Conclusion

Using data obtained from grinding tests performed at 0°C and dynamometer tests performed at the same temperature, it is possible to close the loop between the amount of force and torque required by the RAT motors to grind a rock, and the corresponding current. However, the torque varies greatly with the type of rock that is being grinded. In order to determine the closed loop relationship, a worst-case rock was grinded (hard basalt with flat surface topology). It was found that the worst-case torque required by the

grind motor is 25.13 mNm, the worst-case torque required by the revolve motor is 166.6 mNm, and the worst-case force for the Z-axis motor is 5.907 N.

Using no-load revolve and Z-axis motor data, it was determined that the action of grinding a rock does not contribute greatly to the overall torque/force on the motors. Most of this torque/force is absorbed by friction in the drive trains of these two motors. The revolve motor gear train absorbs approximately 156.8 mNm, while the Z-axis gear train absorbs approximately 4.04 N.

Using motor dynamometer data and the torque required to grind a worst-case scenario rock, the thermal margin was determined for the grind motor, the motor most likely to overheat. It was found that with a temperature limit of 110°C on the rotor, and 85°C on the case, the RE25 motor does overheat at +55°C ambient temperature but does not overheat at an ambient temperature at 35°C after four full hours of grinding. The maximum turn on temperature (MTO) will therefore be specified as 35°C.

The thermal margin was also calculated for the revolve and Z-axis motors in the worst-case scenario that the motors operate continuously, rather than intermittently. It was found that the revolve motor does not overheat at any of the temperature set points with a safety factor of 2.0. It was also found that the Z-axis motor starts to overheat when run in voltage mode (at 8 V) at temperatures below -55°C, at a load of 30 N, and with a safety factor of 2.0. Since the Z-axis motor typically operates between 4 V and 6 V with a load of less than 6 N and a very low duty cycle, this was not seen as a concern.

The revolve and Z-axis motor margins were determined using the no-load current at several different temperature set points (+55°C, +23°C, 0°C, -55°C), since internal losses in the gear trains outweigh the forces and torques due to grinding. Torque and force loads were applied to the revolve and Z-axis motors until the motor current increased to close to double the no-load current. This shows that the motors can overcome the internal losses in the drive train.

Although the Rock Abrasion Tool was specifically developed for the Mars Exploration Rover Mission, the lessons learned during development provide crucial insight for future endeavors. Undoubtedly future missions targeting Mars and other celestial bodies will require drilling and grinding instruments. When specifying design criteria one must be more tolerant of the uncertainties of the unknown targets. System developers must realize the philosophy of designing mechanisms with force and torque margins for a truly unknown target environment should not be overlooked.

## References

1. Hitchiner, M. P., Wilks, E. M., and Wilks, J. "The Polishing of Diamond and Diamond Composite Materials." *Wear*, (1984), pp. 103-119.
2. Gorevan, S. P., Myrick, T., David, K., Chau, J. J., Bartlett, P., Mukherjee, S., Anderson, R., Squyres, S. W., Arvidson, R. E., Madsen, M. B., Bertelsen, P., Goetz, W., Binau, C. S., and Richter, L. "Rock Abrasion Tool: Mars Exploration Rover Mission." *Journal of Geophysical Research*, 108(E12), 8068, doi:10.1029/2003JE002061, in press, 2003.